

1 Article

2 Alginate/chitosan bionanocomposite nanoparticles 3 for pulmonary applications

4 Marcus Hill ¹, Matthew Twigg ², Emer A. Sheridan ³, John G. Hardy ^{4,5,*}, J. Stuart Elborn^{6,*},
5 Clifford C. Taggart ^{2,*}, Christopher J. Scott ^{7,*}, and Marie E. Migaud ^{1,8,*}

6 ¹ School of Pharmacy, Queen's University Belfast Queen's University Belfast, Belfast, BT7 1NN, UK;
7 mhill11@qub.ac.uk (M.H.); mmigaud@health.southalabama.edu (M.E.M.)

8 ² Airway Innate Immunity Group (AiiR), Wellcome Wolfson Institute of Experimental Medicine, School of
9 Medicine, Dentistry and Biomedical Sciences, Queen's University Belfast, 97 Lisburn Road, Belfast, BT9 7BL,
10 Northern Ireland, UK.; m.twigg@qub.ac.uk (M.T.), c.taggart@qub.ac.uk (C.C.T.), c.scott@qub.ac.uk (C.J.S.)

11 ³ Lancashire Teaching Hospitals NHS Trust, Emergency Department, Royal Preston Hospital, Sharoe Green
12 Lane, PR2 9HT, UK; emer.a.barr@gmail.com (E.A.S.)

13 ⁴ Department of Chemistry, Lancaster University, Lancaster, Lancashire, LA1 4YB, UK;
14 j.g.hardy@lancaster.ac.uk (J.G.H.)

15 ⁵ Materials Science Institute, Lancaster University, Lancaster, Lancashire, LA1 4YB, UK;
16 j.g.hardy@lancaster.ac.uk (J.G.H.)

17 ⁶ School of Medicine, Dentistry and Biomedical Sciences, Queen's University Belfast, 97 Lisburn Road,
18 Belfast, BT9 7BL, Northern Ireland, UK; s.elborn@qub.ac.uk (J.S.E.)

19 ⁷ Centre for Cancer Research and Cell Biology, School of Medicine, Dentistry and Biomedical Sciences,
20 Queen's University Belfast, 97 Lisburn Road, Belfast, BT9 7BL, Northern Ireland, UK; c.scott@qub.ac.uk
21 (C.J.S.)

22 ⁸ USA Mitchell Cancer Institute, University of South Alabama, Mobile, AL 36604, USA;
23 mmigaud@health.southalabama.edu (M.E.M.)

24 * Correspondence: j.g.hardy@lancaster.ac.uk (J.G.H.); s.elborn@qub.ac.uk (J.S.E.); c.taggart@qub.ac.uk
25 (C.C.T.); c.scott@qub.ac.uk (C.J.S.); mmigaud@health.southalabama.edu (M.E.M.); Tel.: +1-251-410-4938.

26 Received: date; Accepted: date; Published: date

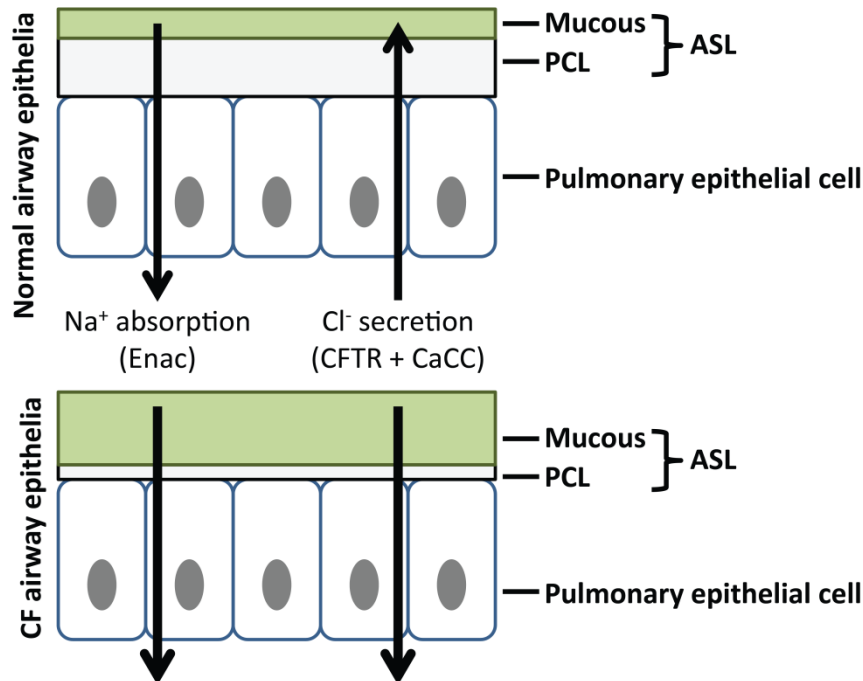
27 **Abstract:** Cystic fibrosis (CF) is a complex, potentially life threatening disease. Here we describe
28 the results of our investigation on the development of alginate/chitosan nanoparticles for
29 pulmonary applications. In the first paradigm, tobramycin loading and release was investigated to
30 treat a clinically relevant model bacteria (*Pseudomonas aeruginosa*) in vitro, and in the second
31 paradigm the nanoparticles were functionalized with secretory leukocyte protease inhibitor (SLPI)
32 which were shown to help inhibit the inflammatory response associated with lung infections and
33 enhance their interactions with mucus in vitro.

34 **Keywords:** biomedical applications; drug delivery systems; nanoparticles; antimicrobial.
35

36 1. Introduction

37 Cystic fibrosis (CF) is a complex, potentially life threatening disease which is manifested
38 through mutations in the cystic fibrosis transmembrane conductance regulator (CFTR) [1]. The
39 protein product of this gene functions as a cyclic AMP (cAMP) dependent transmembrane chloride
40 (Cl⁻) channel. It is responsible for the transport of ions across the apical membrane of exocrine
41 epithelial cells [2]. The protein shows widespread expression across the epithelial lining of most
42 exocrine glands, though is mainly expressed in cells of the small intestine, airways, vas deferens and
43 ducts of the pancreas [3-6]. The mutations present in the CFTR gene have been shown to lead to the
44 subsequent loss of Cl⁻ transport in these cell types. The pulmonary environment has been shown to
45 be one of the most largely effected by the loss of Cl⁻ channel activity [7] concomitant with a decrease
46 in volume of the airway surface liquid (ASL) causing the accumulation of thickened mucus in the

47 pulmonary environment (**Figure 1**) [8,9]. This is believed to increase the susceptibility of the lung to
 48 infection by organisms including *Pseudomonas aeruginosa*, *Haemophilus influenza* and *Staphylococcus*
 49 *aureus* [10]. Early infecting strains such as *S. aureus* are usually cleared by antibiotic therapy though
 50 are believed to facilitate chronic colonization by *P. aeruginosa* [11]. Chronic colonization with *P.*
 51 *aeruginosa* coincides with increasing antibiotic resistance and the emergence of *P. aeruginosa* as the
 52 dominant infecting organism over time [12].



54
 55 **Figure 1.** Events linking altered lung airway surface layer (ASL) volumes to decreased mucociliary
 56 clearance. A) Normal airway surfaces contain a small mucus layer which facilitates entrapment of
 57 inhaled particles and pathogens. ASL autoregulation leads to the maintenance of the periciliary
 58 liquid layer (PCL) which allows movement and clearance of inhaled particles and pathogens. B)
 59 Hyperabsorption of Na^+ and ineffective Cl^- secretion in the CF airway cause depletion of ASL,
 60 collapse of the cilia in the PCL and adherence of concentrated mucus in the airways. Adapted from
 61 [9].

62 Chronic infection with *P. aeruginosa* is one of the most significant events in the pathogenesis of
 63 cystic fibrosis [13]. Tobramycin, is the treatment of choice for those patients with chronic *P.*
 64 *aeruginosa* infection who are deteriorating despite regular colistimethate sodium [14,15]. It is one of
 65 the most effective treatments for pulmonary exacerbations and is generally delivered through
 66 nebulization at a dose of 300 mg twice daily. The pharmacokinetic parameters are similar to other
 67 aminoglycoside drugs resulting in rapid renal excretion [16]. As with other aminoglycosides
 68 tobramycin shows no activity against gram positive organisms such as *S. aureus* therefore early CF
 69 antibacterial therapies often focus on administration of anti-staphylococcal prophylactic antibiotics
 70 [17].

71 Clinical treatment with tobramycin involves twice daily administration of high doses of drug
 72 due to the high absorption and short plasma half-life of the drug [18]. One of the main problems
 73 with CF therapy is non-compliance. Non-compliance with antibiotic regimens can lead to antibiotic
 74 failure [19], therefore altering the dosing schedule of Tobramycin from twice daily to once daily may
 75 in part address compliance issues. Another concern with prolonged tobramycin treatment is the
 76 potential toxicity experienced due to the ototoxic and nephrotoxic property of the drug [20,21].
 77 Nephrotoxicity is often associated with parenteral aminoglycoside therapy but there is limited
 78 evidence of nephrotoxicity and ototoxicity in clinical trials with nebulized tobramycin [22]. With
 79 longer durations of therapy there is an increased potential risk of nephrotoxicity. Therefore the

80 development of delivery systems for tobramycin which could reduce the dosing frequency of the
81 drug while also reducing systemic toxicity upon prolonged exposure may be of clinical benefit.

82 The CF lung provides a further barrier to efficient drug delivery due to the presence of a thick
83 mucus layer on the epithelial lining [23]. This is due to the altered salt transport system within the
84 CF lung which results in increased dehydration and mucus viscosity with delayed mucus clearance
85 [24]. Furthermore, *P. aeruginosa* forms a thick alginate based biofilm which provides increased
86 resistance to antibacterial therapy [11].

87 A further complication arises from the enhanced pro-inflammatory response to infection which
88 causes increased infiltration of neutrophils to the site of bacterial colonization [25]. Neutrophils
89 promote the pro-inflammatory response to infection through the release of various
90 pro-inflammatory proteases such as neutrophil elastase (NE) which can overload the endogenous
91 anti-protease host defenses leading to tissue damage and loss of respiratory function [12]. There is
92 therefore interest in the development of drug delivery systems which can enhance the antibacterial
93 activity of the delivered payload through increased accumulation at the site of infection while
94 reducing the aberrant inflammatory response to infection.

95 The secretory leukocyte protease inhibitor (SLPI) is an 11.7 kDa protein which is naturally
96 expressed as part of the innate immune response in humans [26]. SLPI is naturally expressed in a
97 number of bodily secretions including nasal, pulmonary, salivary and seminal secretions [27-30].
98 SLPI has been shown to display potent anti-inflammatory activity through inhibition of a number of
99 endogenous serine proteases including NE [31]. Due to the high association rate constant for NE it is
100 believed SLPI acts as the primary inhibitor of NE in vivo [12]. Studies have shown therapeutic
101 administration of recombinant SLPI (r-SLPI) to CF patients can reduce the inflammatory response by
102 lowering active levels of NE while also reducing NE mediated IL-8 production which is involved in
103 the recruitment of pro-inflammatory mediators to the site of disease [32,33]. SLPI has also been
104 shown to reduce inflammation through inhibition of NF- κ B signaling [34].

105 Here we describe the results of our investigation on the development of alginate/chitosan
106 nanoparticles for pulmonary applications. In the first paradigm, tobramycin loading and release was
107 investigated, and in the second paradigm the nanoparticles were functionalized with secretory
108 leukocyte protease inhibitor (SLPI) to help inhibit the inflammatory response associated with
109 infection (and potentially passively target the nanoparticles through binding with anionic mucins
110 within mucus to provide enhanced targeting to the site of disease due to its cationic nature).

111 2. Materials and Methods

112 2.1. Materials

113 Unless otherwise noted, all chemicals were obtained from Sigma Aldrich, UK. Boric acid,
114 calcium chloride hexahydrate and the Pierce BCA protein assay kit were purchased from Fisher
115 Scientific UK. Tryptone, sodium chloride (bacteriological grade) and yeast extract were purchased
116 from Oxoid Ltd., Basingstoke, Hampshire, England. Ethanol was purchased from J.T Baker,
117 Netherlands. Recombinant human neutrophil elastase was purchased from the Elastin Products
118 Company (EPC) Owensville, MO, USA. NE substrate
119 (methoxysuccinyl-L-alanyl-alanyl-prolyl-L-valyl-4-nitroanilide) was purchased from Calbiochem,
120 USA. Recombinant human secretory leukocyte protease inhibitor (SLPI) was purchased from
121 Amgen UK. Biotinylated anti-human SLPI antibody was purchased from R&D Systems (Abingdon,
122 Oxon, UK). Sputum from CF patients was obtained anonymously from the adult CF centre at Belfast
123 City Hospital. Sputum samples were in excess to requirements for diagnostic purposes. Permission
124 to use sputum samples (which would have been disposed of) for validation purposes was given by
125 the Director of R&D in Belfast Health and Social Care Trust.

126 2.2. Preparation of tobramycin loaded alginate/chitosan nanoparticles

127 Several formulations of tobramycin were tested for their ability to formulate tobramycin loaded
128 nanoparticles with no aggregation. CaCl₂ and chitosan were utilized as cationic crosslinkers.

129 Tobramycin was included in all formulations. Briefly, aqueous solutions of tobramycin (1.5 mg in 3
130 ml) were added to various amounts of sodium alginate (pH 5.4) while stirring (500 rpm) at room
131 temperature. 1 ml of chitosan (1% v/v glacial acetic acid, pH 5.1) at various concentrations was
132 added while stirring (500 rpm). The nanoparticles were collected by centrifugation at 20,000 g and
133 washed in PBS three times by centrifugation resuspension cycles.

134 2.3. Nanoparticle characterization

135 The size and zeta potential analysis of the nanoparticles was determined by dynamic light
136 scattering (DLS) using a Malvern Zetasizer (Nano ZS; Malvern instruments, Malvern U.K). For
137 particle analysis each sample was read in triplicate (10 runs each). The average of three separate
138 samples was taken and the data presented as the mean \pm standard deviation. Transmission electron
139 microscopy (TEM) was performed using a JEOL JEM1400 transmission electron microscope at an
140 accelerating voltage of 80 kV. Nanoparticles (0.6 mg/ml) were loaded on a copper grid
141 (Formvar/Carbon 200 μ m mesh, Agar Scientific), the moisture wicked off and allowed to dry. 2 μ l of
142 uranyl acetate (2% w/v) was added to provide contrast between the nanoparticles and copper grid.

143 2.4. Conjugation of SLPI to chitosan

144 Chitosan 0.5 ml (2 mg/ml, in 1% v/v glacial acetic acid) was diluted 1:1 in PBS buffer (25 mM,
145 pH 7.4) and 10 μ l of SLPI was added (25 mg/ml). The pH of the solution was adjusted to 5 and the
146 conjugation was initiated by the addition of 1-ethyl-3-(dimethylaminopropyl carbodiimide) (EDC)
147 (2.5 mg/ml) and left stirring for 6 h at room temperature. The SLPI/chitosan conjugate was used
148 instantly for nanoparticle formation with alginate and excess EDC was removed by washing of the
149 nanoparticles through centrifugation resuspension cycles.

150 2.5. Quantification of SLPI conjugation

151 Nanoparticles were formulated as described previously and centrifuged at 20,000 g. The
152 supernatant was collected. Blank nanoparticles (not conjugated to SLPI) were also included as a
153 control. The levels of SLPI conjugation achieved were measured with the BCA assay kit (Pierce, UK).
154 25 μ l of control and conjugate nanoparticles were added to 175 μ l of BCA reagent A (sodium
155 carbonate, sodium bicarbonate, bicinchoninic acid and sodium tartrate in 0.1 M sodium hydroxide)
156 and B (4% W/W cupric sulphate in water) in a 96 well plate. The plate was then incubated for 60 min
157 at 37°C. The absorbance of the resultant solution was read at 570 nm and compared to a calibration
158 curve of SLPI.

159 2.6. Analytical methodology for detection of tobramycin sulphate

160 Reagent A consisting of 80 mg of ortho-phthaldialdehyde in 1ml of 95% ethanol and reagent B
161 containing 200 μ l of boric acid (pH 9.7, 0.4 M), 400 μ l β -mercaptoethanol and 200 μ l of diethyl ether
162 were mixed. Serial dilutions of tobramycin were prepared in boric acid (pH 9.7, 0.4 M). 100 μ l of each
163 tobramycin standard was added to 100 μ l of the reagent mixture. The plate was read by fluorescence
164 at $\lambda_{ex}/\lambda_{em}$ 360/460 nm, respectively.

165 2.7. Quantification of tobramycin release

166 Drug release was quantified by incubating the nanoparticles in dialysis membranes with a
167 10,000 Da MWCO at 37°C with agitation. The release of the tobramycin was quantified by incubating
168 3 mg of nanoparticles in 1 ml of PBS in the donor compartment with 5 ml of PBS in the receiver
169 compartment. At each time point the PBS was collected and replaced with fresh PBS release
170 medium. Quantification of the tobramycin release was performed by diluting the release medium
171 1:1 with Boric acid (0.4 M pH 9.7) prior to derivatization with ortho-phthaldialdehyde (80 mg) in a
172 solution containing 1 ml of 95% ethanol, 200 μ l Boric acid (0.4 M pH 9.7), 400 μ l of
173 β -mercaptoethanol and 200 μ l diethyl ether. The fluorescent derivative was monitored by
174 fluorescence at $\lambda_{ex}/\lambda_{em}$ 360/460 nm, respectively.

175 2.8. Minimum inhibitory concentration effect of tobramycin on *P. aeruginosa*

176 Broth micro-dilution tests were performed according to NCCLS guide lines. Serial two-fold
177 dilutions of tobramycin (from stock solution which had been sterile filtered with 0.22 µm filter) in
178 100 µl of Luria Bertani (LB) broth were performed on a 96 well plate in the range 0-25 µg/ml for the
179 drug loaded nanoparticles, free tobramycin and the blank nanoparticles as negative control. The
180 actively growing cultures were diluted to an optical density reading of 0.3 (A550) to give a starting
181 inoculum of 2×10^5 CFU/ml. 100 µl of the starting inoculum (2×10^5 CFU/ml) was added to each well of
182 the plate and incubated aerobically at 37°C for 24 h. Positive and negative controls were included in
183 each assay.

184 2.9. Inhibition of neutrophil elastase by SLPI functionalised alginate/chitosan nanoparticles

185 Anti-neutrophil elastase activity was monitored by incubation with the human neutrophil
186 elastase (HNE) specific substrate methoxysuccinyl-Ala-Ala-Pro-Val-P-nitroanilide (Sigma, Aldrich,
187 UK). Inhibitions of HNE (Elastin products, Owensville, MO) were measured in the presence and
188 absence of both blank and SLPI conjugated nanoparticles. The assay was carried out by incubating
189 10 µl (10 mg/ml particles) of blank and SLPI conjugated nanoparticles containing 100 µg/ml SLPI
190 with 4 µl of HNE (100 µg/ml). HNE activity was measured by the cleavage of chromogenic
191 methoxysuccinyl-Ala-Ala-Pro-Val-P-nitroanilide substrate by adding 50 µl of 0.2 mM substrate in
192 0.1 M HEPES buffer containing 0.5 M NaCl. Assays were conducted at 37°C and the formation of the
193 fluorescent product (p-nitroaniline) was measured continuously at 405 nm on a BMG-Labtech
194 Fluorstar Optima fluorescent plate reader.

195 2.10. Preparation of Rhodamine 6G loaded alginate/chitosan nanoparticles

196 3 ml of a tobramycin stock solution in water (0.5 mg/ml) was added to 3 ml of sodium alginate
197 (3 mg/ml pH 5.4). 250 µl of Rhodamine 6G (2 mg/ml) was then added to the tobramycin alginate
198 mixture. 1 ml of chitosan (1% v/v glacial acetic acid pH 5.1) was added while stirring (500 rpm). The
199 nanoparticles were collected by centrifugation at 20,000 g and washed in PBS three times by
200 centrifugation resuspension cycles.

201 2.11. Penetration of SLPI functionalised nanoparticles in CF mucus

202 The penetration of rhodamine loaded nanoparticles with and without SLPI functionalisation
203 was studied in CF mucus. A 500 µl layer of 10% gelatin (Porcine type A Sigma- Aldrich) was added
204 to a 24 well microplate and allowed to harden. 500 µl of CF sputum or PBS control was added and
205 allowed to settle. 200 µl of SLPI functionalised nanoparticles (10 mg/ml) were added to the sputum
206 and PBS control wells with SLPI at a concentration of 100 µg/ml. Non-conjugated rhodamine loaded
207 nanoparticles were diluted to give an equivalent concentration of rhodamine. Particle penetration
208 was measured over 24 h after which the gelatin layers were washed (PBS x 6) and the gelatin was
209 melted and fluorescence measured at 480/520 nm. Penetration in CF mucus was measured by
210 comparison to the PBS control which was measured as 100% penetration. Fluorescent values were
211 analysed in reference to Rhodamine 6G standards in the range (0-1000 ng/ml).

212 2.12. Statistical analysis

213 Results were analysed with GraphPad Prism, version 5.03, GraphPad Software (San Diego,
214 USA). T-test and one-way ANOVA analyses were performed. Statistical significance critical values
215 were defined as **P < 0.01, ***P < 0.0001.

216 3. Results and Discussion

217 We have an interest in the development of nanoparticles designed for therapeutic application in
218 diseases such as Cystic Fibrosis (CF) [35].

219 3.1. Nanoparticle preparation and tobramycin loading and release

220 Various microparticle-/nanoparticle-based drug delivery systems have been developed to
 221 facilitate the effective delivery of drugs to the pulmonary system [36]. Here we report the
 222 development of tobramycin-loaded nanoparticles composed of alginate and chitosan. The results of
 223 varying the ratio of the components (alginate:chitosan:tobramycin:CaCl₂) on particle formation are
 224 reported in **Table 1**.

225 **Table 1.** Optimisation of formulation parameters in the design of alginate/chitosan nanoparticles.
 226 Results presented as mean ± S.D, N = 3.

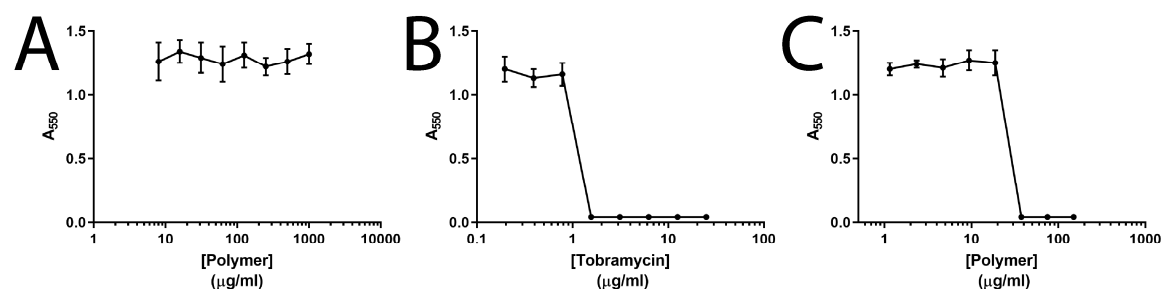
Alginate (w/w ratio)	Chitosan (w/w ratio)	Tobramycin (w/w ratio)	CaCl ₂ (w/w ratio)	Aggregation
9	1.5	1.5	3	Yes
9	1.5	1.5	0.8	Yes
9	0.8	0.8	0	No
9	1	3	0	Yes
9	1	1.5	0	No

227
 228 During the optimization studies we observed that a higher concentration of cations in the
 229 formulation resulted in the aggregation of the nanoparticles (**Table 1**). The optimal formulation of
 230 alginate:chitosan:tobramycin 9:1:1.5 (w/w/w), resulted in the formation of nanoparticles with a fairly
 231 narrow size distribution and high loading of tobramycin (**Table 2, Figure S1 and Figure S2**) and was
 232 therefore used for further studies. The nanoparticle size distribution assessed by DLS measurements
 233 (**Table 2, Figure S1**) were somewhat larger than those observed by TEM (**Figure S2**), however, the
 234 DLS data was judged to be more representative of the whole population of nanoparticles.

235 **Table 2.** Properties of the nanoparticles prepared with the optimal formulation of
 236 alginate:chitosan:tobramycin (9:1:1.5, w/w/w). Results presented as mean ± S.D, N = 3.

Particle size (nm)	PDI	Zeta potential (mV)	Tobramycin loading in nanoparticles (µg/mg)	% entrapment
437.5 ± 22.3	0.27 ± 0.07	21.6 ± 1.1	74.2 ± 3.4	44.5 ± 2.0

237
 238 Tobramycin loading (**Table 2**) and release (**Figure S3**) was quantified by fluorimetry after
 239 derivatization of the tobramycin with ortho-phthalaldehyde [37] (the calibration curve is depicted
 240 in **Figure S4**); a typical biphasic release was observed with 18.9% of the entrapped tobramycin
 241 released within the first 24 h, although the overall release was limited to 25.4% of the total amount of
 242 loaded tobramycin over the course of the experiment. The optimal formulation of the
 243 tobramycin-loaded alginate/chitosan nanoparticles was tested against live cultures of *P. aeruginosa*
 244 (**Figure 2**). The unloaded nanoparticles showed no activity against *P. aeruginosa*, tobramycin alone
 245 had an MIC of 1.5 µg/ml, and the tobramycin-loaded nanoparticles showed activity in a dose
 246 dependent manner as expected (with a somewhat elevated MIC of 6.25 µg/ml which is likely to be
 247 due to the rate of diffusion of tobramycin from the nanoparticles).
 248



249

250

251

252

Figure 2. MIC analysis of tobramycin-loaded alginate/chitosan nanoparticles against *P. aeruginosa*. A) Unloaded nanoparticle control. B) Free tobramycin. C) Tobramycin loaded nanoparticles. Mean values \pm S.D, N = 3.

253

3.2. SLPI-conjugated nanoparticle preparation and interactions with model biological milieu

254

255

256

257

258

259

260

261

262

Disease states such as CF are characterized by increased infiltration of pro-inflammatory cytokines in the lung [25] which leads to extensive tissue damage through NE mediated activity [12]. As a natural inhibitor of NE [31] it was anticipated that the conjugation of SLPI to the nanoparticles could potentially inhibit NE mediated tissue destruction while also achieving passive targeting for the particles. The properties of nanoparticles prepared with SLPI in the absence/presence of carbodiimide crosslinker are displayed in **Table 3** (and **Figure S5**), with nanoparticles formed in the absence of carbodiimide containing 0.2 μg of SLPI, whereas those formed in the presence of carbodiimide containing 11.2 μg of SLPI, highlighting the necessity of using the carbodiimide to attach the SLPI to the nanoparticles.

263

264

Table 3. Nanoparticle properties following preparation without/with carbodiimide. Results presented as mean \pm S.D, N = 3.

Crosslinker (EDC)	Particle size (nm)	PDI	Zeta potential (mV)	Conjugated SLPI (μg) in nanoparticles (mg), ($\mu\text{g}/\text{mg}$)
No	437.5 \pm 26.5	0.26 \pm 0.09	-22.9 \pm 3.1	0.2 \pm 0.3
Yes	458.0 \pm 31.1	0.31 \pm 0.12	-19.2 \pm 2.1	11.2 \pm 2.3

265

266

267

268

269

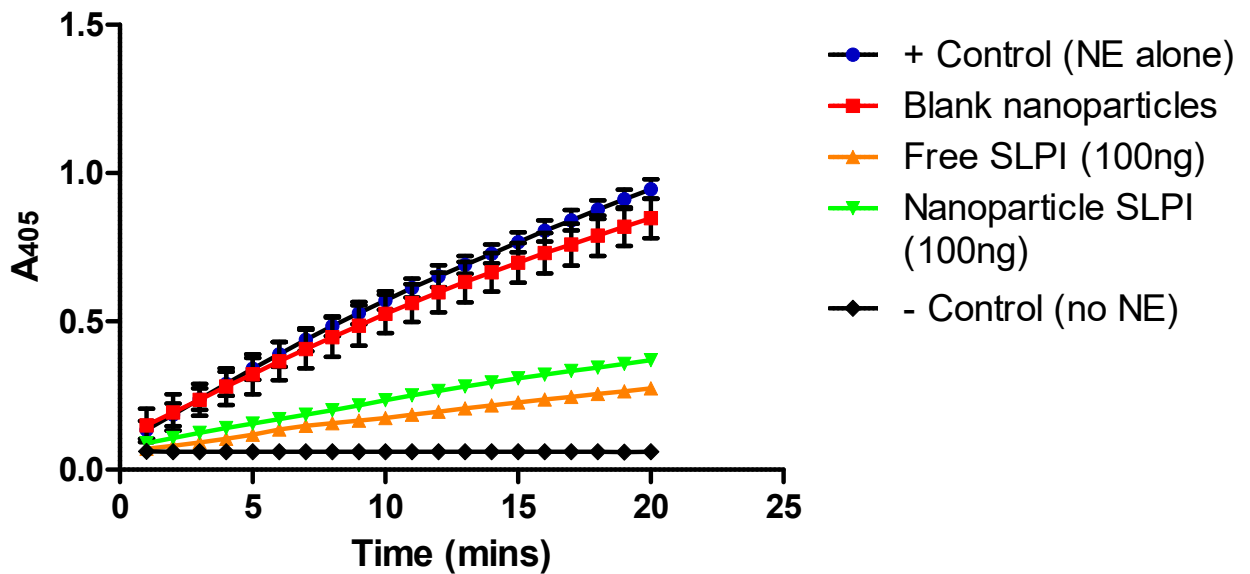
270

271

272

273

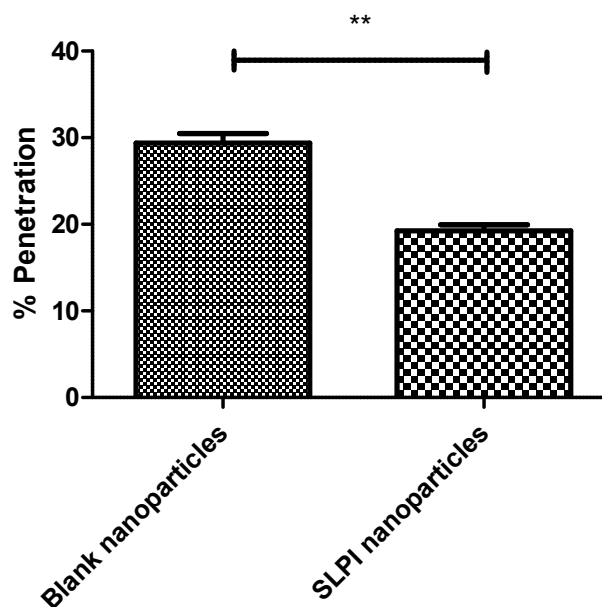
To evaluate whether any of the conjugated SLPI was functional after conjugation to the chitosan in the nanoparticles, the SLPI-conjugated nanoparticles were incubated with human neutrophil elastase (NE) and their ability to inhibit the cleavage of a chromogenic substrate (methoxysuccinyl-Ala-Ala-Pro-Val-P-nitroanilide) was studied [38] and compared to free SLPI and unmodified nanoparticles (**Figure 3**). The unmodified/blank alginate/chitosan nanoparticles show very little NE inhibitory activity (similar to NE alone), by contrast the SLPI conjugated particles displayed a similar level of activity as the free SLPI, confirming that the SLPI retains NE inhibitory activity when conjugated to the nanoparticles.



274
275

Figure 3. Inhibition of NE by SLPI-conjugated nanoparticles. Results presented as mean \pm S.D, N = 3.

276 In order to effectively treat *P. aeruginosa* infections it is necessary for drugs to achieve
 277 therapeutic concentrations at the site of bacterial colonization. *P. aeruginosa* has been shown to reside
 278 within the thick mucus secretions within the CF lung [39]. We anticipated the conjugation of SLPI to
 279 the nanoparticles could enhance their mucoadhesive properties via electrostatic interactions [40].
 280 The penetration of SLPI-conjugated nanoparticles into CF mucus was assessed using
 281 rhodamine-loaded nanoparticles (**Figure 4 and Figure S6**) in accordance with a literature protocol
 282 [41]. We observed that the SLPI conjugated nanoparticles entrapping rhodamine dye were retained to
 283 a greater level in CF sputum over the non-conjugated particles. Only 19.4% of nanoparticles
 284 functionalised with SLPI were shown to traverse CF mucus as opposed to 29.7% of particles without
 285 SLPI (in line with literature showing nanoparticles with cationic coatings could be retained within
 286 the pulmonary environment longer, thereby increasing the therapeutic efficacy of the drug) [42].
 287



288
289
290

Figure 4. Ability of rhodamine loaded nanoparticles to penetrate CF mucus. Mean \pm S.D, N = 3, (**P<0.01).

291 5. Conclusions

292 The complexity of CF treatment regimens has been shown to be largely responsible for patient
293 non-compliance [19,43], and the formulation of nanoparticles displaying mucoadhesive properties is
294 a potential solution to minimizing problems associated with non-compliance, with potentially
295 significant beneficial economic, health and societal impacts at the global scale. The nanoparticles
296 described herein were capable of delivering a potent antimicrobial (tobramycin) to *P. aeruginosa*, and
297 the conjugation of SLPI enhanced their mucoadhesive properties [39, 42] potentially increasing the
298 efficacy of drug delivery over prolonged periods, and potentially thereby helping minimize
299 problems associated with non-compliance after successful pre-clinical and clinical studies [44,45].

300 **Supplementary Materials:** The following are available online at www.mdpi.com/xxx/s1, Figure S1. DLS
301 analysis of the nanoparticles prepared with the optimal formulation of alginate:chitosan:tobramycin (9:1:1.5,
302 w/w/w). Figure S2. TEM analysis of alginate/chitosan nanoparticles. Figure S3. Cumulative release of
303 tobramycin release from alginate/chitosan nanoparticles. Figure S4. Calibration curve for tobramycin sulphate
304 in nanoparticle supernatant following formulation of tobramycin loaded alginate/chitosan nanoparticles.
305 Figure S5. Calibration curve for SLPI in the range (31.25 – 500 µg/ml) quantified with the BCA assay kit (Pierce,
306 UK). Figure S6. Standard curve of Rhodamine 6G in the concentration range (0-1000 ng/ml).

307 **Author Contributions:** Conceptualization, C.C.T., C.J.S., J.S.E., and M.E.M.; methodology, all authors; formal
308 analysis, all authors; investigation, all authors; data curation, M.H., M.E.M.; writing—original draft
309 preparation, M.H. and J.G.H.; writing—review and editing, all authors; supervision, M.E.M.; project
310 administration, M.E.M.; funding acquisition, M.E.M.

311 **Funding:** This research was supported by: a PhD studentship from Queen’s University Belfast for M.H.;
312 Lancaster University for a Faculty of Science and Technology Early Career Internal Grant to support
313 collaborative interactions between J.G.H. and M.E.M.; a MRC Proximity to Discovery grant (MC_PC_17192) for
314 supporting interactions with J.G.H. and E.A.S.; the UK Engineering and Physical Sciences Research Council
315 (EPSRC, EP/H031065/1) to support C.C.T., C.J.S., J.S.E and M.E.M and an Innovate UK Knowledge Transfer
316 Partnership to support M.T. The APC was funded by M.E.M. at the University of South Alabama.

317 **Acknowledgments:** We thank Professor Colin McCoy for access to a BMG-Labtech Fluorstar Optima
318 fluorescent plate reader.

319 **Conflicts of Interest:** The authors declare no conflict of interest. The funders had no role in the design of the
320 study; in the collection, analyses, or interpretation of data; in the writing of the manuscript, and in the decision
321 to publish the results.

322 References

- 323 1. Dulhanty, A. M.; Chang, X. B.; Riordan, J. R. Mutation of potential phosphorylation sites in the
324 recombinant R domain of the cystic fibrosis transmembrane conductance regulator has significant effects
325 on domain conformation. *Biochem. Biophys. Res. Commun.* **1995**, *206*, 207–214. DOI: 10.1006/bbrc.1995.1029.
- 326 2. Riordan, J. R.; Rommens, J. M.; Kerem, B.; Alon, N.; Rozmahel, R.; Grzelczak, Z.; Chou, J. L. Identification
327 of the cystic fibrosis gene: cloning and characterization of complementary DNA. *Science* **1989**, *245*, 1066–73.
328 DOI: 10.1126/science.2475911.
- 329 3. Marino, C. R.; Matovcik, L. M.; Gorelick, F. S.; Cohn, J. A. Localization of the cystic fibrosis transmembrane
330 conductance regulator in pancreas. *J. Clin. Invest.* **1991**, *88*, 712–6. DOI: 10.1172/JCI115358.
- 331 4. Jacquot, J.; Puchelle, E.; Hinnrasky, J.; Fuchey, C.; Bettinger, C.; Spilmont, C.; Pavirani, A. Localization of
332 the cystic fibrosis transmembrane conductance regulator in airway secretory glands. *Eur. Resp. J.* **1993**,
333 *6*, 169–76.
- 334 5. Sbarbati, A.; Bertini, M.; Catassi, C.; Gagliardini, R.; Osculati, F. Ultrastructural lesions in the small bowel
335 of patients with cystic fibrosis. *Ped. Res.* **1998**, *43*, 234–9. DOI: 10.1203/00006450-199804001-01393.
- 336 6. Kreda, S. M.; Mall, M.; Mengos, A.; Rochelle, L.; Yankaskas, J.; Riordan, J. R.; Boucher, R. C.
337 Characterization of wild-type and deltaF508 cystic fibrosis transmembrane regulator in human respiratory
338 epithelia. *Mol. Biol. Cell*, **2005**, *16*, 2154–67. DOI: 10.1091/mbc.e04-11-1010.
- 339 7. Krouse, M. E. Is cystic fibrosis lung disease caused by abnormal ion composition or abnormal volume? The
340 *J. Gen. Physiol.* **2001**, *118*, 219–22.

- 341 8. Stenbit, A. E.; Flume, P. A. Pulmonary exacerbations in cystic fibrosis. *Curr. Opin. Pulm. Med.* **2011**, *17*, 442–
342 7. DOI: 10.1097/MCP.0b013e32834b8c04.
- 343 9. Mall M.; Boucher R. Pathogenesis of Pulmonary Disease in Cystic Fibrosis. In *Cystic Fibrosis in the 21st*
344 *Century*. Bush A.; Alton, E. W. F. W.; Davies, J.C.; Griesenbach, U.; Jaffe, A., Eds; Prog Respir Res.
345 Karger: Basel, Switzerland, **2006**; Volume 34, pp. 116-121, ISBN: 978-3-8055-7960-5.
346 DOI:10.1159/000088489.
- 347 10. Haley, C. L.; Colmer-Hamood, J. A.; Hamood, A. N. Characterization of biofilm-like structures formed by
348 *Pseudomonas aeruginosa* in a synthetic mucus medium. *BMC Microbiol.*, **2012**, *12*, 181. DOI:
349 10.1186/1471-2180-12-181.
- 350 11. May, T. B.; Shinabarger, D.; Maharaj, R.; Kato, J.; Chu, L.; DeVault, J. D.; Rothmel, R. K. Alginate synthesis
351 by *Pseudomonas aeruginosa*: a key pathogenic factor in chronic pulmonary infections of cystic fibrosis
352 patients. *Clin. Microbiol. Rev.* **1991**, *4*, 191–206. DOI: 10.1128/cmr.4.2.191.
- 353 12. Quinn, D. J.; Weldon, S.; Taggart, C. C. Antiproteases as therapeutics to target inflammation in cystic
354 fibrosis. *Open Respir. Med. J.*, **2010**, *4*, 20–31. DOI: 10.2174/1874306401004010020.
- 355 13. Høiby, N.; Ciofu, O.; Bjarnsholt, T. *Pseudomonas aeruginosa* biofilms in cystic fibrosis. *Future Microbiol.*
356 **2010**, *5*, 1663–74. DOI: 10.2217/fmb.10.125.
- 357 14. Cystic fibrosis: diagnosis and management. Available online:
358 [https://www.nice.org.uk/guidance/ng78/chapter/Recommendations#pulmonary-monitoring-assessment-a](https://www.nice.org.uk/guidance/ng78/chapter/Recommendations#pulmonary-monitoring-assessment-and-management)
359 [nd-management](https://www.nice.org.uk/guidance/ng78/chapter/Recommendations#pulmonary-monitoring-assessment-and-management) (accessed on 30 06 2019).
- 360 15. Tobramycin. Available online: <https://bnf.nice.org.uk/drug/tobramycin.html> (accessed on 30 06 2019).
- 361 16. Omri, A.; Beaulac, C.; Bouhajib, M.; Montplaisir, S.; Sharkawi, M.; Lagacé, J. Pulmonary retention of free
362 and liposome-encapsulated tobramycin after intratracheal administration in uninfected rats and rats
363 infected with *Pseudomonas aeruginosa*. *Antimicrob. Agents Chemother.* **1994**, *38*, 1090–5. DOI:
364 10.1128/AAC.38.5.1090.
- 365 17. Smyth, A.; Walters, S. Prophylactic antibiotics for cystic fibrosis. *Cochrane Database Syst. Rev.* **2003**, *3*,
366 CD001912. DOI: 10.1002/14651858.CD001912.
- 367 18. Girón Moreno, R. M.; Salcedo Posadas, A.; Mar Gómez-Punter, R. Inhaled antibiotic therapy in cystic
368 fibrosis. *Archivos de Bronconeumología*, **2011**, *47*, 14–8. DOI: 10.1016/S0300-2896(11)70031-X.
- 369 19. IM2 Cystic Fibrosis Patient Adherence (Adult).
370 <https://www.england.nhs.uk/wp-content/uploads/2016/11/im2-cystic-fibrosis-patient-adherence.pdf>
371 (accessed on 30 06 2019).
- 372 20. Selimoglu, E. Aminoglycoside-induced ototoxicity. *Curr. Pharm. Des.* **2007**, *13*, 119–26. DOI:
373 10.2174/138161207779313731.
- 374 21. Kumin, G. D. Clinical Nephrotoxicity of Tobramycin and Gentamicin. *JAMA*, **1980**, *244*, 1808. DOI:
375 10.1001/jama.1980.03310160024018.
- 376 22. Tobramycin 300 mg/ 5 ml nebuliser solution. Available online:
377 <https://www.medicines.org.uk/emc/product/2683/smpc> (accessed on 30 06 2019).
- 378 23. Ramphal, R.; Lhermitte, M.; Filliat, M.; Roussel, P. The binding of anti-pseudomonal antibiotics to
379 macromolecules from cystic fibrosis sputum. *J. Antimicrob. Chemother.* **1988**, *22*(4), 483–90. DOI:
380 10.1093/jac/22.4.483.
- 381 24. Mall, M.; Grubb, B. R.; Harkema, J. R.; O’Neal, W. K.; Boucher, R. C. Increased airway epithelial Na+
382 absorption produces cystic fibrosis-like lung disease in mice. *Nature Medicine*, **2004**, *10*, 487–93. DOI:
383 10.1038/nm1028.
- 384 25. Heeckeren, A.; Walenga, R.; Konstan, M. W.; Bonfield, T.; Davis, P. B.; Ferkol, T. Excessive inflammatory
385 response of cystic fibrosis mice to bronchopulmonary infection with *Pseudomonas aeruginosa*. *J. Clin.*
386 *Invest.* **1997**, *100*, 2810–5. DOI: 10.1172/JCI119828.
- 387 26. King, A. E.; Critchley, H. O.; Kelly, R. W. Presence of secretory leukocyte protease inhibitor in human
388 endometrium and first trimester decidua suggests an antibacterial protective role. *Mol. Hum. Reprod.* **2000**,
389 *6*, 191–6. DOI: 10.1093/molehr/6.2.191.
- 390 27. Appelhans, B.; Ender, B.; Sachse, G.; Nikiforov, T.; Appelhans, H.; Ebert, W. Secretion of antileucoprotease
391 from a human lung tumor cell line. *FEBS Lett.* **1987**, *224*, 14–18. DOI: 10.1016/0014-5793(87)80413-1.
- 392 28. Franken, C.; Meijer, C. J.; Dijkman, J. H. Tissue distribution of antileucoprotease and lysozyme in humans.
393 *J. Histochem. Cytochem.* **1989**, *37*, 493–8. OI:10.1177/37.4.2926127.

- 394 29. Heinzl, R.; Appelhans, H.; Gassen, G.; Seemüller, U.; Machleidt, W.; Fritz, H.; Steffens, G. Molecular
395 cloning and expression of cDNA for human antileukoprotease from cervix uterus. *Eur. J. Biochem.* **1986**,
396 *160*, 61–7. DOI: 10.1111/j.1432-1033.1986.tb09940.x.
- 397 30. Lee, C. H.; Igarashi, Y.; Hohman, R. J.; Kaulbach, H.; White, M. V.; Kaliner, M. A. Distribution of secretory
398 leukoprotease inhibitor in the human nasal airway. *Am. Rev. Respir. Dis.* **1993**, *147*, 710–6. DOI:
399 10.1164/ajrccm/147.3.710.
- 400 31. Thompson, R. C.; Ohlsson, K. Isolation, properties, and complete amino acid sequence of human secretory
401 leukocyte protease inhibitor, a potent inhibitor of leukocyte elastase. *Proc. Natl. Acad. Sci. USA* **1986**, *83*,
402 6692–6. DOI: 10.1073/pnas.83.18.6692.
- 403 32. McElvaney, N. G.; Nakamura, H.; Birrer, P.; Hébert, C. A.; Wong, W. L.; Alphonso, M.; Crystal, R. G.
404 Modulation of airway inflammation in cystic fibrosis. In vivo suppression of interleukin-8 levels on the
405 respiratory epithelial surface by aerosolization of recombinant secretory leukoprotease inhibitor. *J. Clin.*
406 *Invest.* **1992**, *90*, 1296–301. DOI: 10.1172/JCI115994.
- 407 33. McElvaney, N. G.; Doujajji, B.; Moan, M. J.; Burnham, M. R.; Wu, M. C.; Crystal, R. G. Pharmacokinetics of
408 recombinant secretory leukoprotease inhibitor aerosolized to normals and individuals with cystic fibrosis.
409 *Am. Rev. Respir. Disease*, **1993**, *148*, 1056–60. DOI: 10.1164/ajrccm/148.4_Pt_1.1056.
- 410 34. Taggart, C. C.; Cryan, S.-A.; Weldon, S.; Gibbons, A.; Greene, C. M.; Kelly, E.; McElvaney, N. G. Secretory
411 leukoprotease inhibitor binds to NF-kappaB binding sites in monocytes and inhibits p65 binding. *J. Exp.*
412 *Med.* **2005**, *202*, 1659–68. DOI: 10.1084/jem.20050768.
- 413 35. Hill, M.; Cunningham, R. N.; Hathout, R. M.; Johnston, C.; Hardy, J. G.; Migaud, M. E. Formulation of
414 antimicrobial tobramycin loaded PLGA nanoparticles via complexation with AOT. *Journal of Functional*
415 *Biomaterials.* **2019**, *10*, 26.
- 416 36. Mansour, H. M.; Rhee, Y.-S.; Wu, X. Nanomedicine in pulmonary delivery. *Int. J. Nanomed.* **2009**, *4*, 299–
417 319. DOI: <https://doi.org/10.2147/IJN.S4937>.
- 418 37. Benson, J. R.; Hare, P. E. O-phthalaldehyde: fluorogenic detection of primary amines in the picomole
419 range. Comparison with fluorescamine and ninhydrin. *Proc. Natl. Acad. Sci. USA* **1975**, *72*, 619–22. DOI:
420 10.1073/pnas.72.2.619.
- 421 38. Weldon, S.; McNally, P.; McElvaney, N. G.; Elborn, J. S.; McAuley, D. F.; Wartelle, J.; Taggart, C. C.
422 Decreased levels of secretory leukoprotease inhibitor in the Pseudomonas-infected cystic fibrosis lung are
423 due to neutrophil elastase degradation. *J. Immunol.* **2009**, *183*, 8148–56. DOI: 10.4049/jimmunol.0901716.
- 424 39. Baltimore, R. S.; Christie, C. D.; Smith, G. J. Immunohistopathologic localization of Pseudomonas
425 aeruginosa in lungs from patients with cystic fibrosis. Implications for the pathogenesis of progressive
426 lung deterioration. *Am. Rev. Respir. Dis.* **1989**, *140*, 1650–61. DOI: 10.1164/ajrccm/140.6.1650.
- 427 40. Hirano, M.; Kamada, M.; Maegawa, M.; Gima, H.; Aono, T. Binding of human secretory leukocyte
428 protease inhibitor in uterine cervical mucus to immunoglobulins: pathophysiology in immunologic
429 infertility and local immune defense. *Fertil. Steril.* **1999**, *71*, 1108–14. DOI: 10.1016/S0015-0282(99)00142-9.
- 430 41. Ungaro, F.; d'Angelo, I.; Coletta, C.; d'Emmanuele di Villa Bianca, R.; Sorrentino, R.; Perfetto, B.; Quaglia,
431 F. Dry powders based on PLGA nanoparticles for pulmonary delivery of antibiotics: modulation of
432 encapsulation efficiency, release rate and lung deposition pattern by hydrophilic polymers. *J. Control.*
433 *Release*, **2012**, *157*, 149–59. DOI: 10.1016/j.jconrel.2011.08.010.
- 434 42. Yamamoto, H.; Kuno, Y.; Sugimoto, S.; Takeuchi, H.; Kawashima, Y. Surface-modified PLGA nanosphere
435 with chitosan improved pulmonary delivery of calcitonin by mucoadhesion and opening of the
436 intercellular tight junctions. *J. Control. Release* **2005**, *102*, 373–81. DOI: 10.1016/j.jconrel.2004.10.010.
- 437 43. Dodd, M. E., & Webb, A. K. Understanding non-compliance with treatment in adults with cystic fibrosis. *J.*
438 *R. Soc. Med.* **2000**, *93*, 2–8.
- 439 44. Fisher, J. T.; Zhang, Y.; Engelhardt, J. F. Comparative biology of cystic fibrosis animal models. *Methods Mol.*
440 *Biol.* **2011**, *742*, 311–34. DOI: 10.1007/978-1-61779-120-8_19.
- 441 45. Pezzulo, A. A.; Tang, X. X.; Hoegger, M. J.; Alaiwa, M. H. A.; Ramachandran, S.; Moninger, T. O.; Zabner,
442 J. Reduced airway surface pH impairs bacterial killing in the porcine cystic fibrosis lung. *Nature* **2012**, *487*,
443 109–13. DOI: 10.1038/nature11130.

